

Characteristic temperature in magnetically doped amorphous semiconductors

E. Helgren, J. J. Cherry, L. Zeng, and F. Hellman

Department of Physics, University of California San Diego, La Jolla, California 92093, USA

(Received 9 December 2004; published 22 March 2005)

The introduction of magnetic moments such as Gd into amorphous Si produces dramatic effects in electrical transport below a characteristic temperature T^* . Below T^* , the conductivity of the magnetically doped systems is strongly suppressed compared to equivalent nonmagnetic Y doped samples, and displays enormous negative magnetoresistance. T^* occurs at relatively high temperatures (~ 10 – 100 K) and decreases sharply with increasing Gd concentration, passing smoothly through the metal-insulator transition. In ternary samples with both Gd and nonmagnetic Y, T^* decreases strongly with increasing metallization, whether due to the addition of Gd alone or a mixture of Gd and Y. These results cannot be explained by simple magnetic interaction models, suggest the crucial role of electron screening and are reminiscent of mass enhancement behavior.

DOI: 10.1103/PhysRevB.71.113203

PACS number(s): 75.50.Pp, 71.23.Cq, 71.30.+h, 75.70.-i

Amorphous metal-semiconductor alloys (a - M -Si) offer unique insight into the metal insulator transition (MIT) as a comparison to doped crystalline materials. It has been widely documented that amorphous alloys undergo a MIT with identical low temperature behavior but at much greater dopant concentration compared to their crystalline counterparts due to significant additional disorder. The doping of local magnetic moments into semiconductors near the MIT causes dramatic effects in the magnetic and transport properties, including enormous negative magnetoresistance, field-dependent anomalous (nonspectral weight conserving) optical conductivity, and a magnetic susceptibility with a near-Curie law temperature dependence but a nonmonotonic dependence on composition, including a large peak at the MIT.^{1–3} The enormous magnetic field dependence has allowed measurements of scaling behavior continuously through the 3D MIT on a single sample, including tunneling determination of the electron density of states.^{4,5}

Strong similarities exist between the a - M -Si systems studied here and both dilute magnetic semiconductor systems (DMS), such as (Ga,Mn)As and the perovskite manganites. In all these systems, there are indications of strong coupling of electrical conductivity, magnetic properties, and even the structural or lattice system, suggesting the possibility of an all-encompassing theoretical description. Distinct differences in our system, e.g., the strong disorder, and magnetic moments from f rather than d -shell electrons, offer unique insights into the underlying physics. In these systems the separate control of electron and moment concentrations is critical to understanding the underlying physics.

While there has been some success in describing the low temperature properties of amorphous doped semiconductors on both the metallic and insulating sides of the MIT, including the magnetically doped semiconductors,^{6–8} a strikingly unresolved question is the nature of the higher temperature behavior where the effects upon the charge carriers due to the magnetic dopants “turns on.” This temperature, which we call T^* , is clearly seen in a sharp decrease of dc conductivity $\sigma_{dc}(T)$ for the magnetically doped a -Gd-Si alloys below that of a comparable nonmagnetic a -Y-Si and also reflects an upper limit of significant magnetoresistance. A magnetic

temperature in our system analogous to the Curie temperature, T_C , found in DMS materials would be the spin glass freezing temperature, T_f . However T^* represents a fundamentally different magnetic thermal energy scale, i.e., the onset of interactions between the moments and the charge carrying electrons (whereas T_C or T_f sets the temperature where the moments interact), and in fact T^* will be shown here to follow a different trend with dopant concentration, indicating underlying physics unique from that of T_f . T^* has been noted in previous work;^{1,9} however, the dependence on carrier and moment concentration, from which an understanding of the essential interactions can be developed, was not determined. In this work, we study the effects of separate tuning of charge carrier and magnetic dopant concentration, as well as the semiconducting matrix. We find a strong dependence of T^* on metallicity (independent of magnetic moment concentration) and on the semiconductor band gap. These results are strongly suggestive that the crucial factor in determining T^* is the electron screening of magnetic moments.

Samples of amorphous Gd_xSi_{1-x} , Gd_xGe_{1-x} and $Gd_xY_ySi_{1-x-y}$ across a broad range of dopant concentrations about the MIT were made by electron beam co-evaporation at a base pressure of 10^{-9} Torr onto SiN-coated Si substrates held at or below 70°C . Film thicknesses vary between 1000 and 4000 Å with the thicknesses determined by profilometry. Rutherford backscattering verified the thicknesses and was used to determine the film concentrations. Further details on sample preparation and characterization can be found in the literature.⁹ DC conductivity data from room temperature to as low as 300 mK for some measurements were taken using a routine four probe technique.

Figure 1(a) shows $\sigma_{dc}(T)$ for several metallic a -Gd-Si samples and data for the critical concentration, $x_c \cong 14$ at. %. A sharp downturn at T^* is clearly visible. Linear axes are used to emphasize the linear temperature behavior of the conductivity at high temperatures. Figure 1(b) shows $\sigma_{dc}(T)$ on logarithmic axes for a -Gd₁₄Si₈₆ and a -Y₁₅Si₈₅. This pair was chosen because from room temperature to ≈ 100 K, their conductivity curves fall on top of each other. Below this temperature range, a sharp deviation in the con-

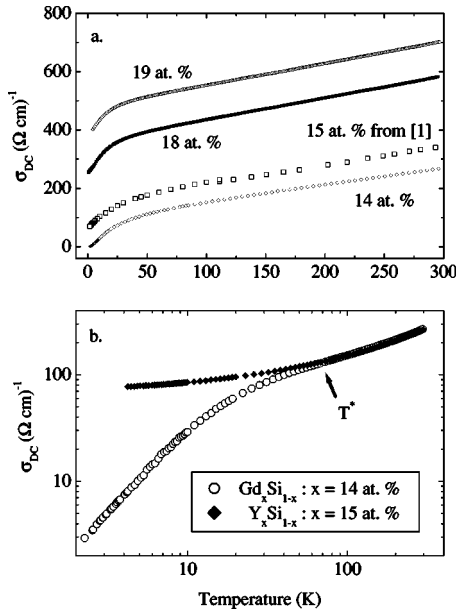


FIG. 1. (a) dc conductivity vs T for metallic $a\text{-Gd}_x\text{Si}_{1-x}$. (b) σ_{dc} vs T on loglogarithmic axes for $a\text{-Gd}_{14}\text{Si}_{86}$ and $a\text{-Y}_{15}\text{Si}_{85}$; high temperature data fall on top of each other indicating identical conduction mechanisms, but low temperature data deviate dramatically below T^* .

ductivity of the magnetically doped $a\text{-Gd-Si}$ from its nonmagnetic counterpart $a\text{-Y-Si}$ is clearly visible. The temperature at which the deviation occurs is defined as T^* . Both Gd and Y in virtually all materials are trivalent with nearly identical ionic radii. Thus, that the high temperature behavior of σ_{dc} is identical in these two systems is not surprising. While Y^{3+} is nonmagnetic though, Gd^{3+} is characterized by $J=S=7/2$ and $L=0$ due to the half-filled f shell. The deviation of $\sigma_{dc}(T)$ at T^* , and the physics below this temperature, must be due to the interactions between the magnetic ions and the carriers.

While T^* is most obviously defined by the difference between σ_{YSi} and σ_{GdSi} , it was not possible to obtain samples that were perfectly matched for all compositions. Instead, a functional form appropriate to nonmagnetic samples on the metallic side of the MIT was used:

$$\sigma_{dc}(T) = \sigma_0 + AT^{1/2} + BT^{p/2}, \quad (1)$$

where σ_0 is a residual $T=0$ term, the second term arises from corrections due to electron-electron effects, and the last term is due to the effects of weak localization, with $p=2$ in the case of phonon scattering.¹⁰ Equation (1) has been used for doped crystalline and amorphous semiconductors.^{1,11,12} At high temperatures, despite being out of a region of strict validity, this equation is still a good parametrization as justified by the quality of the fit, e.g., Eq. (1) accurately fits the $a\text{-Y-Si}$ data shown in Fig. 1 across the entire measured temperature range.

The samples of $a\text{-Gd-Si}$ measured from room temperature to 300 mK fit Eq. (1) very well at high temperatures and, as seen previously, at low temperatures.⁵ At intermediate temperatures the fit fails completely, due to the sharp drop in

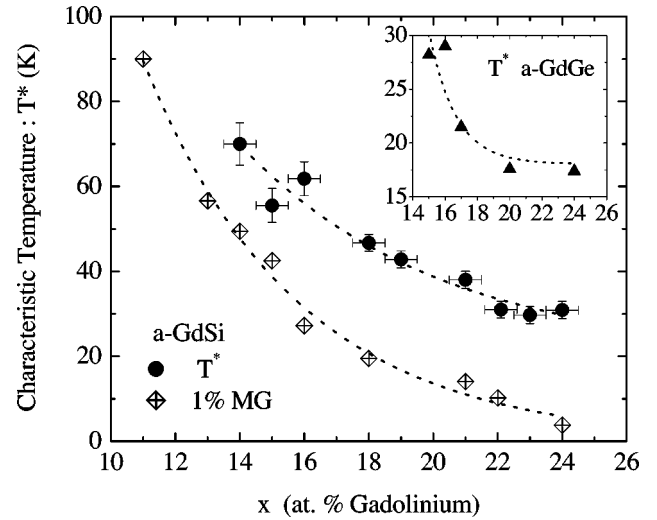


FIG. 2. T^* and 1% MG vs Gd concentration x for $a\text{-Gd}_x\text{Si}_{1-x}$. The inset shows T^* for $a\text{-Gd}_x\text{Ge}_{1-x}$. Dotted lines are guides to the eye.

$\sigma_{dc}(T)$ at T^* . The deviation from the high temperature form of Eq. (1) (dominated by BT) is therefore used to determine T^* . We chose as a criterion a $4(\Omega \text{ cm})^{-1}$ difference; different criteria including a % deviation did not significantly change the results.

The characteristic temperature T^* for $a\text{-Gd-Si}$ and $a\text{-Gd-Ge}$ across a broad range of dopant concentrations is shown in Fig. 2. Perhaps unexpectedly, the data shows a strong decrease of T^* with increasing Gd concentration. T^* is substantially reduced in the Ge matrix, but shows the same decrease with increasing metallicity.

We were unable to determine a T^* for insulating samples ($x < 0.14$). At low temperatures transport for insulating samples is via variable range hopping (VRH), but crosses over to a functional form akin to Eq. (1) at higher temperatures, obscuring the precipitous break in $\sigma_{dc}(T)$ which is so obvious in the metallic samples. Due to this crossover, we were unable to devise a rigorous analysis method that fit insulating $a\text{-Y-Si}$ $\sigma_{dc}(T)$ at all temperatures, and therefore could not differentiate between the onset of magnetic effects and VRH.

We have also measured the magnetoconductance (MG) and find an identical trend of decreasing MG with increasing Gd concentration. Figure 3 shows MG for 6 T applied field (defined at each temperature and for each composition as $[\sigma(6T) - \sigma(0)]/\sigma(0)$ for $a\text{-Gd-Si}$ for compositions on both the insulating and metallic side of the MIT. By choosing a fixed value of MG, such as 1% (the horizontal line shown in Fig. 3), the temperature at which the MG reaches this criterion decreases with increasing x (shown in Fig. 2). With MG we are able to continue the study on the insulating side of the MIT and find that the trend continues smoothly through the MIT.

To better understand the driving mechanism behind the trends seen in Fig. 2, we studied a set of ternary samples $\text{Gd}_x\text{Y}_y\text{Si}_{1-x-y}$, in which the magnetic moment concentration can be controlled independently of the charge carrier concentration. By fixing the Gd concentration, x and varying Y

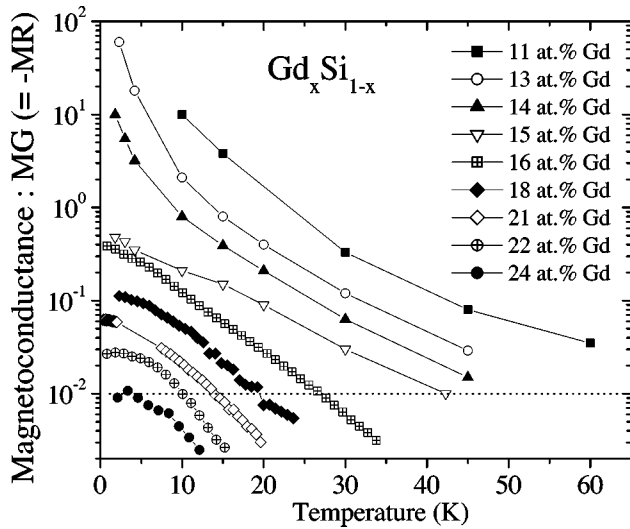


FIG. 3. Magnetoconductivity MG of $a\text{-Gd}_x\text{Si}_{1-x}$ vs T . $MG \equiv [\sigma(6T) - \sigma(0)] / \sigma(0) = -\text{magnetoresistance (MR)}$ in the usual definition of $MR \equiv [\rho(6T) - \rho(0)] / \rho(6T)$. The dotted line demarks $MG = 1\%$. The temperature at which the curves cross the 1% line decreases with increasing x similar to T^* .

concentration y , we hold the magnetic impurity concentration constant while increasing the charge carrier concentration. The magnitude of $\sigma_{dc}(T)$ increased with increasing $x+y$ as expected. Comparable magnitudes of $\sigma_{dc}(300\text{ K})$ for different samples with constant $x+y$ (including $y=0$) were observed, consistent with the expectation that the electron concentration scales monotonically with $x+y$.¹³

Figure 4 shows T^* for a number of ternary samples, including the $y=0$ data from Fig. 2, plotted vs. total dopant concentration $x+y$ measured from the critical concentration

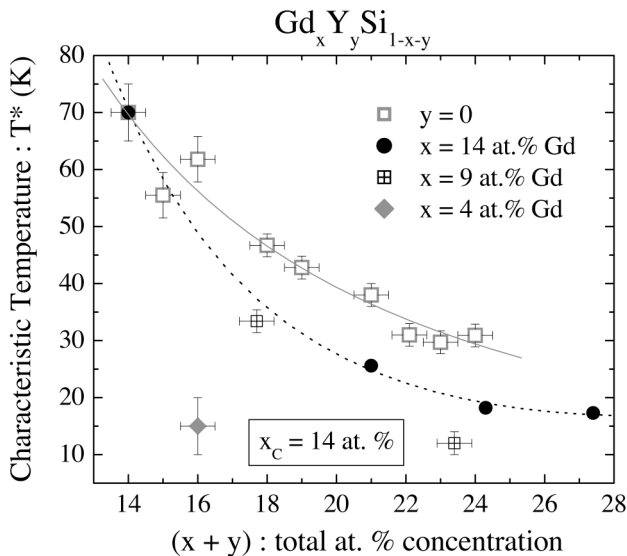


FIG. 4. T^* for ternary $a\text{-Gd}_x\text{Y}_y\text{Si}_{1-x-y}$ vs $x+y$ measured from critical MIT concentration $x_c=0.14$ Gd. Open squares are $a\text{-Gd}_x\text{Si}_{1-x}$ (i.e., $y=0$) from Fig. 2. Black circles and dotted lines show the trend of four ternary samples with constant $x \approx 0.14$ Gd, and varying Y concentration y . Two crossed squares are constant $x \approx 0.09$ Gd; the gray diamond is $x \approx 0.04$ Gd, $y = 0.12$ Y.

at the MIT (x or $y=0.14$). T^* decreases strongly for increasing $x+y$, whether that increase is due to increasing x at $y=0$ or constant magnetic dopant concentration $x \approx \text{const}$ and increasing y (e.g., the dotted line for Gd $x \approx 0.14$ and the crossed squares for $x \approx 0.09$). Since $\sigma_{dc}(T)$ increases monotonically with total $x+y$, we take this data to show that T^* decreases with increasing electron concentration. Considering samples with constant total electron concentration $x+y \approx \text{const}$ (i.e., vertical lines in Fig. 4), for decreasing x we find a trend of decreasing T^* . T^* thus decreases strongly on adding electrons, whether from adding Gd or Y. Adding Y drops it farther and faster than adding Gd, as the latter adds both more electrons and magnetic dopants (see the lines of constant $x+y$ and the $x \approx 0.04$ diamond in Fig. 4).

This dependence is surprising: if the onset of magnetic effects were directly related to the energy associated with a single electron-local moment interaction such as the exchange interaction J_{sf} , it should be independent of Gd concentration. If the onset were related to the energy associated with Gd-Gd magnetic interactions, which leads to spin glass freezing, T^* should increase with increasing Gd concentration, as does the freezing temperature T_f .³ We suggest that the explanation for the decrease in T^* with increasing Gd or Y concentration must lie in electron screening which is reduced by the development at low temperatures of the Coulomb correlation gap; specifically that the interactions between local magnetic moments and itinerant electrons are screened with increasing efficiency when the number of conduction electrons relative to the number of magnetic impurity sites increases due to the reduced correlation gap in more metallic samples. This idea is supported by the decrease of T^* in $a\text{-Gd-Ge}$ relative to $a\text{-Gd-Si}$. The dielectric constant, a measure of the potential for screening, is directly related to the band gap, which is smaller in Ge.

A characteristic temperature T^* has been observed in DMS systems such as $\text{Cd}_{1-x}\text{Mn}_x\text{Se}$,¹¹ which are doped crystalline semiconductor systems but has not been systematically investigated. For the crystalline DMS, this thermal energy scale occurs at a much lower value than in the amorphous systems studied here, but higher energy scales in amorphous systems are typical (presumably as a consequence of the orders of magnitude higher electron concentration at the MIT which causes all energies to be larger and hence thermal energy to be comparatively lower). The sharp decrease in $\sigma_{dc}(T)$ at T^* seen in DMS systems has been interpreted as an onset of scattering from bound magnetic polarons (BMP).¹⁴ We do not believe that this is the correct interpretation of our results as BMP are not a good description of our system due to the high ratio (of order 1) of conduction electrons to magnetic dopant sites (in DMS this ratio is orders of magnitude less).

The most successful means to model data in the temperature range near T^* , while maintaining the general framework of Eq. (1) which works so well at high and low temperatures, is to make the residual conductivity, σ_0 , temperature dependent. In their analysis of DMS, Dietl *et al.*^{11,14} use this approach, and incorporate a temperature dependent σ_0 into Eq. (1). The turning on of magnetic interactions and the resulting temperature dependence of the otherwise temperature independent quantity σ_0 is reminiscent of mass enhancement

seen in heavy fermion (HF) systems.¹⁵ In HF systems though this turning on of interactions causes an *increase* in σ_{dc} (due to an accompanying scattering rate renormalization which compensates for the increased mass), while here it causes a *decrease* presumably because the mean free path is already limited to an interatomic spacing (and even samples on the metallic side of the MIT are not accurately described by Boltzmann transport theory with a scattering rate). This mass enhancement is likely developing at low temperatures as the Coulomb gap develops and the magnetic moments are less effectively screened.

The agreement between our experimental results and theoretical predictions for ferromagnetic (FM) DMS materials indicates a strong link between these two types of systems. In Ref. 16 a theoretical model for FM in DMS systems, is discussed and although the magnetic ground state of our Gd based materials is a spin glass,³ the author indicates that above the magnetic ordering temperature, some mass renormalization due to dressing will occur. Optical measurements on *a*-Gd-Si and *a*-Y-Si show a change in spectral weight, $N_{eff}(\omega)$, as a function of temperature and field that might indicate mass renormalization.² In Ref. 16 a model is described in which an up-spin electron propagating between magnetic dopant sites will experience a dressing, due to Coulomb repulsion (of nearby sites occupied with a down spin). This explanation is consistent with our observation that T^* decreases in the Ge matrix (with a higher dielectric constant than in Si) and upon increasing the electron dopant concentration (which improves the efficiency of screening). Further qualitative agreement with theory is found in the observed positive magnetoconductance predicted in both Refs. 8 and 16. In Ref. 8 FM semiconductor systems with localized charge carriers are studied, taking into account high defect concentrations. These authors predict regions of correlated magnetic dopant spins, e.g., “puddles,” and when a magnetic field is applied to such a system, the spins in the puddle regions would align and enhance the transport. This theory

maps well onto our system with its high disorder.

In terms of other possible explanations, it is unlikely that the Kondo effect plays a role, both because of the large 7/2 spin of the Gd and because the Gd *f* levels are far from the Fermi energy. Thus the Kondo temperature should be very low and should increase with increasing dopant concentration opposite to the trend we see in T^* .

In summary, dc conductivity investigations across a broad range of dopant concentrations for two semiconducting matrices have systematically determined the onset energy scale at which magnetic interactions become important in doped amorphous magnetic semiconductors. We observe a strong *decrease* in this energy scale with *increasing* electron concentration, indicating that screening or correlation effects must play an important role. These trends in the characteristic temperature can be directly related to other systems that show such linked electrical and magnetic behavior, namely DMS (Ga,Mn)As and the perovskite manganites.

We are encouraged by recent theoretical attempts to incorporate magnetic interactions, electron-electron interactions, and disorder in such systems,^{6,8} but a self-consistent model describing the magneto-transport spanning the complete range of temperatures is still lacking. Our results highlight the interplay of magnetic interactions and electron-electron interactions in magnetically doped systems near the MIT, i.e., neither magnetic dopant concentration alone or electron dopant concentration alone solely determines the suppression of conductivity and onset of enormous MG in these magnetic semiconductors.

ACKNOWLEDGMENTS

We would like to thank R. C. Dynes, L. Bokacheva, K. Steinmeyer, K. Adams, and K. McCarthy for useful discussions and help with data; B. Culbertson for RBS; D. Smith for TEM. This research was supported by the NSF, DMR-0203907.

¹F. Hellman, M. Q. Tran, A. E. Gebala, E. M. Wilcox, and R. C. Dynes, Phys. Rev. Lett. **77**, 4652 (1996).

²D. N. Basov, A. M. Bratkovsky, P. F. Henning, B. Zink, F. Hellman, Y. J. Wang, C. C. Homes, and M. Strongin, Europhys. Lett. **57**, 240 (2002).

³F. Hellman, D. R. Queen, R. M. Potok, and B. L. Zink, Phys. Rev. Lett. **84**, 5411 (2000).

⁴W. Teizer, F. Hellman, and R. C. Dynes, Phys. Rev. B **67**, 121102(R) (2003).

⁵W. Teizer, F. Hellman, and R. C. Dynes, Phys. Rev. Lett. **85**, 848 (2000).

⁶P. Majumdar and S. Kumar, Phys. Rev. Lett. **90**, 237202 (2003).

⁷A. S. Alexandrov and A. M. Bratkovsky, Phys. Rev. Lett. **84**, 2043 (2000).

⁸A. Kaminski and S. Das Sarma, Phys. Rev. B **68**, 235210 (2003).

⁹M. Liu and F. Hellman, Phys. Rev. B **67**, 054401 (2003).

¹⁰P. A. Lee and T. V. Ramakrishnan, Rev. Mod. Phys. **57**, 287 (1985).

¹¹C. Leighton, I. Terry, and P. Becla, Phys. Rev. B **58**, 9773 (1998).

¹²G. A. Thomas, A. Kawabata, Y. Ootuka, S. Katsumoto, S. Kobayashi, and W. Sasaki, Phys. Rev. B **26**, 2113 (1982).

¹³The Hall effect is too small to measure for these samples with their large *n* at any distance from the MIT.

¹⁴T. Dietl and J. Spałek, Phys. Rev. B **28**, 1548 (1983); T. Dietl, M. Sawicki, T. Wojtowicz, J. Jaroszynski, W. Plesiewicz, L. Swierkowski, and J. Kossut, in *Anderson Localization*, edited by T. Ando and H. Fukuyama (Springer-Verlag, Berlin, 1988), p. 58.

¹⁵L. Degiorgi, Rev. Mod. Phys. **71**, 687 (1999).

¹⁶J. E. Hirsch, Phys. Rev. B **62**, 14 131 (2000).